DOI: 10.1002/ejic.200500439

Synthesis, Crystal Structures and Photoluminescence of Mercury(II) Complexes with Two Homologous Novel Functional Rigid Ligands

Hong-Ping Zhou,[a,b] Yu-Peng Tian,*[a,c,d] Jie-Ying Wu,[a] Ju-Zhou Zhang,[a] Dong-Mei Li,[a] Yong-Min Zhu,[a] Zhang-Jun Hu,[a] Xu-Tang Tao,[c] Min-Hua Jiang,[c] and Yi Xie*[b]

Keywords: Mercury / Functional rigid ligands / X-ray diffraction / Luminescence

Two novel functional rigid ligands, 2,2′- and 4,4′-bipyridyl-based "building blocks", 9-ethyl-3,6-bis[2-(4-pyridyl)ethenyl]carbazole ($\mathbf{L^1}$) and 9-ethyl-3,6-bis[2-(2-pyridyl)ethenyl]-carbazole ($\mathbf{L^2}$), were synthesized. Treatment of $L^{1,2}$ as "building blocks" with $Hg(SCN)_2$ or HgI_2 afforded helixes, macrocycles, and chains, which can be further self-assembled by a π–π stacking interaction, hydrogen bond, and interatomic force in the solid state to form two-dimensional networks. In complexes **1**–**4**, Hg^{II} centers all adopt four-coordination modes in different coordination environments, but they present different architectures with slightly adjusted structures of the ligands and counteranions, indicating that the nature of the ligand and anion plays an important role in the coordination networks. The luminescent properties of compounds **1**–**4** have been studied.

Introduction

In the past decade, more and more attention has been focused on the crystal design and engineering of multidimensional arrays and networks containing metal ions as nodes because of the potential application of such molecular materials in catalysis, electronics, molecular sensing, magnetic devices, and porous and nanosize materials.[1,2] The rational design and construction of metal–organic frameworks, with their fascinating structures and potential properties, continues to attract interest in current supramolecular chemistry.[3] Up to now, extensive studies have been carried out to give many novel one- (1D), two- (2D), and three-dimensional (3D) frameworks based on the assembly of metal salts with rigid *N*,*N*′- donor ligands, such as 4,4′-bipyridine or 2,2′-bipyridine and their derivatives. Bridging bis(pyridyl) ligands are often used in the construction of metal-containing macromolecules, and the geometry of the bis(pyridyl) ligand can define the primary structure of the self-assembled macromolecule through metal-coordination, hydrogen bonds and π–π stacking interactions.[4] However, some organic ligands with special functionality for supramolecular architectures and functional compounds, because of synthetic difficulties, have been reported rarely to date.

On the other hand, carbazole compounds, as is well known, exhibit good hole transporting properties and their charge transporting complexes can create free carriers in the visible region through the photocarrier generation process.[5] Recently, carbazole-containing compounds have been extensively studied for the application of an electroluminescent (EL) device and fabrication of light-emitting diodes (LED)[6] because of their sufficient hole/electron transporting and luminescent properties. However, the devices are mostly organic compounds or polymers, and the low melting points or low decomposition temperatures inhibit their applications. Functionalization of the organic molecule (addition of donor atoms, e.g. N or O) to allow incorporation into inorganic/organic coordination complexes can offer the advantages of high thermal stability and solvent resistance compared to all-organic materials. So we have tried to design and synthesize functional ligands 9-ethyl-3,6-bis[2-(4-pyridyl)ethenyl]carbazole ($\mathbf{L^1}$) and 9-ethyl-3,6-bis[2-(2-pyridyl)ethenyl]carbazole ($\mathbf{L^2}$). Interestingly, by the careful design of rigid ligands containing carbazole cores and bipyridyl, we were able to obtain complexes with functionally different structures. Furthermore, mercury(II) complexes have been extensively studied because of their structural diversities and attractive optical properties such as photoluminescence and nonlinear optical effects.[7] In this article, we present a series of mercury(II) complexes containing the new functional rigid ligands $\mathbf{L^1}$ and $\mathbf{L^2}$ (Scheme 1). Slightly adjusting the structure of the

[a] Department of Chemistry, Anhui University,
Hefei 230039, P.R. China
E-mail: yptian@ahu.edu.cn
[b] Department of Chemistry, University of Science and Technology of China,
Hefei 230026, P.R. China
E-mail: yxie@ustc.edu.cn
[c] State Key Laboratory of Crystal Materials, Shandong University,
Jinan 250100, P.R. China
[d] State Key Laboratory of Coordination Chemistry, Nanjing University,
Nanjing 210093, P.R. China

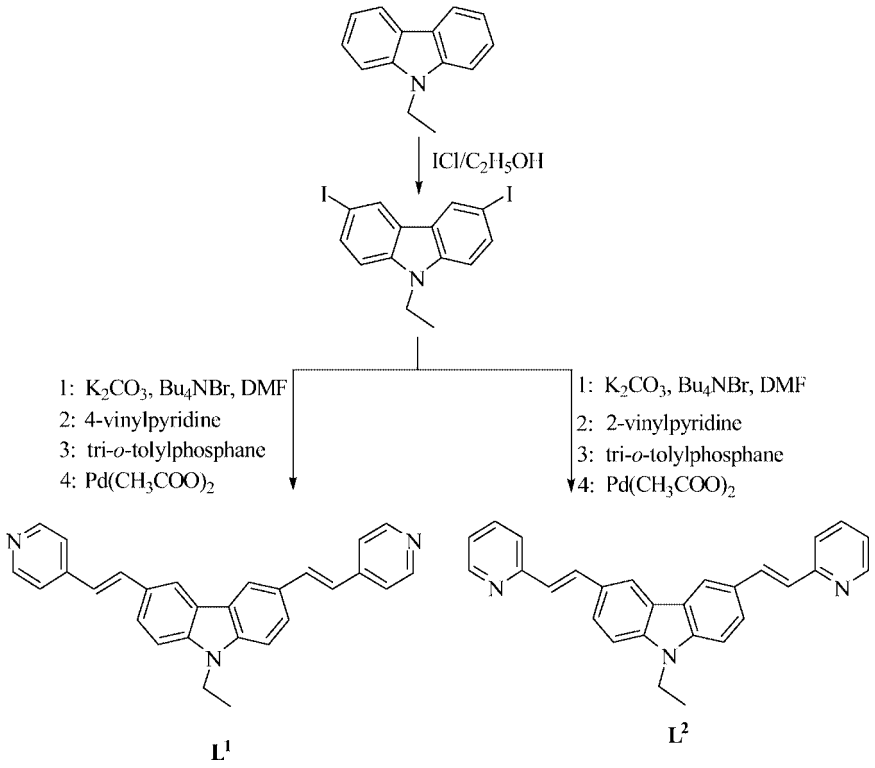

Scheme 1. Synthesis of ligands $\mathbf{L^1}$, $\mathbf{L^2}$.

ligands and counteranions gives potential changes to form different architectures. Here the syntheses, structures, photoluminescence and high thermal stability properties of mercury(II) complexes are reported.

Results and Discussion

All of the compounds are stable in air and insoluble in water or in common organic solvents. High yields of the products indicate that these compounds are thermodynamically stable under the prevailing reaction conditions. IR spectra of the same counteranion compounds are similar, compounds **1** and **3** showing strong absorption bands at about 2065 and 2061 cm^{-1} respectively that are diagnostic of coordinated sulfocyan; middle absorption bands at about 419 and 420 cm^{-1} respectively that are the Hg–N stretching frequencies; and middle absorption bands at about 327 and 328 cm^{-1} respectively that are the Hg–S stretching frequencies. Compounds **2** and **4** show middle absorption bands at about 420 and 419 cm^{-1} respectively that are the Hg–N stretching frequencies and strong absorption bands at about 151 cm^{-1} that are the Hg–I stretching frequencies.

Crystal Structures

In many previous examples, the Hg^{II} cation was found to act as a tetrahedral node with a coordination angle of about 90° to generate 1-D, 2-D, and 3-D structures.[7] It has recently been reported that macrocycles, polymers, or sheets resulted from the reaction of a pyridine spacer with an angle of 120° and a metal node with an angle of 90°.[7] Thus, the reaction of $\mathbf{L^1}$ and $\mathbf{L^2}$ with $Hg(SCN)_2$ and HgI_2 was anticipated to afford 1-D, 2-D, and 3-D structures bearing metallacyclic or metallamacrocyclic analogous structures.

The reaction of equimolar amounts of the bis(pyridine) ligands $\mathbf{L^1}$ and $\mathbf{L^2}$ (Scheme 1) and mercury(II) halide or sulfocyanate gave the corresponding complexes **1**–**4**. These compounds were isolated as analytically pure, air-stable, yellow or red solids that are very sparingly soluble in common organic solvents such as chloroform, dichloromethane, and tetrahydrofuran. Complexes **1**–**4** were characterized by X-ray structure determinations.

Crystal Structure of $[HgL^1(SCN)_2]_n$ (1)

By the slow diffusion of MeOH solution of $Hg(SCN)_2$ into a solution of $\mathbf{L^1}$ in CH_2Cl_2, red crystalline **1** was obtained. Its formulation, $[Hg(\mathbf{L^1})(SCN)_2]_n$, was confirmed by elemental analysis and the use of the single-crystal X-ray diffraction method. The X-ray structural analysis revealed the formation of single-stranded helical chain structures. Each Hg^{II} center exhibits a distorted tetrahedral coordination geometry with two pyridines from $\mathbf{L^1}$ and two sulfur atoms of $Hg(SCN)_2$ as anticipated (Figure 1, a). The bond angles around the mercury atom are in the range 98.67(14)–127.06(6)°, indicating a quite distorted tetrahedral geometry. The coordinated pyridine rings are perpendicularly twisted relative to each other, presumably to minimize the steric hindrance between them.

It is shown in part a of Figure 1 that the ligand takes on the *cis*-conformation in this structure to connect two crystallographically different Hg^{II} ions. Two pyridine rings

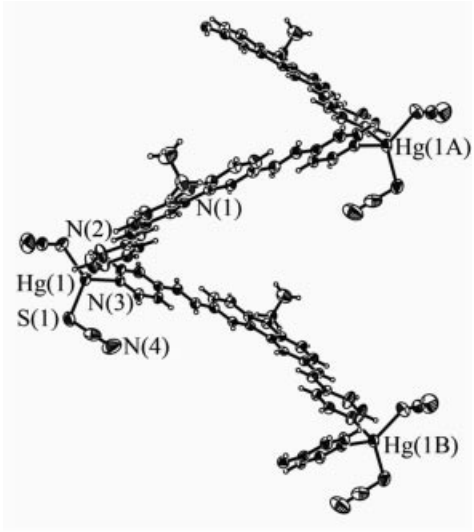

(a)

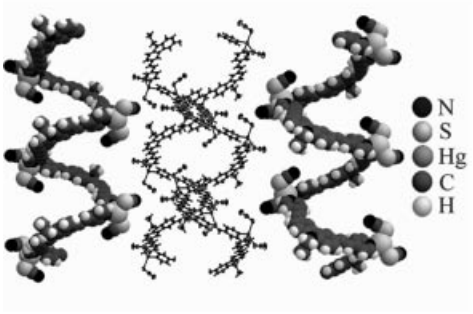

(b)

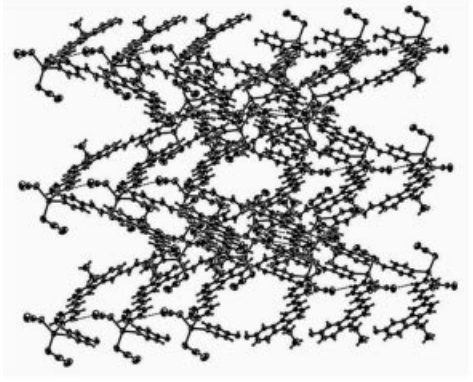

(c)

Figure 1. (a) Molecular structure of **1** showing different coordination environments of the two structurally independent Hg^{II} ions. (b) Space-filling plots of the right-handed chain (left), left-handed chain (right), and the ball-and-stick plot (middle) of the double helix bridged by a π–π stacking interaction in complex **1**. (c) Molecular packing of complex **1**.

are connected by Hg(1) to adopt the same orientation, while those connected by Hg(1A) take on the opposite orientation. This connectivity extends the span of the two ligands and forces a turn in the chain. Such an arrangement endows the chain structure with an intrinsic helical sense. The repeating unit in this single-stranded helix consists of a pair consisting of the $Hg(SCN)_2$ unit and the ligand. As depicted in part b of Figure 1, a fairly flattened, loose helix runs along the *b* axis with a pitch of about 7.99 Å (distance between the two mercury centers at the same phase); at the widest point the diameter of the helix equals 16.03 Å. Left-handed helicates connect through an intermolecular π–π stacking interaction between phenyl and pyridine rings with the short distance of 3.38 Å, and there is some evidence of a weak interaction between each nitrogen atom of $Hg(SCN)_2$ and the pyridyl C–H group of a molecule in an adjacent chain (C–H···N = 3.24 Å);[4] right-handed helicates also connect in this way (Figure 1, c). Unlike most double-helical complexes,[9] the adjacent left-handed and neighboring right-handed helical chains are not entangled together but interact through π–π stacking interactions with the short distance of 3.24 Å as illustrated in Figure 1 (parts b and c), which may contribute to stabilizing the formation of the helical structure. Then a two-dimensional network is formed through the C–H···N hydrogen bond interaction established between ligands and thiocyanate anions of adjacent chains and intermolecular π–π stacking interactions. Because left-handed and right-handed helical chains coexist in the crystal structure, the whole crystal is mesomeric and does not exhibit chirality.

Crystal Structure of $Hg(L^1)_2I_2$ (2)

The crystal contains individual $Hg(\mathbf{L^1})_2I_2$ neutral molecules. A perspective drawing with atom-labeling scheme is shown in Figure 2 (a). Each metal atom is tetracoordinated by two N donors from different ligands and two terminal iodine atoms of HgI_2. The Hg–N distance (Table 1) in the complex is in the range of those found in the other complexes;[7] Hg–I distances are also in the range of those found in other Hg^{II} iodine complexes with terminal Hg–I bonds.[7] The bond angles N(2A)–Hg(1)–N(2), N(2A)–Hg(1)–I(1), N(2)–Hg(1)–I(1) and I(1)–Hg(1)–I(1A) are 76.3(3), 105.10(2), 106.74(2) and 139.18(3)°, respectively. Table 1 shows that the Hg–N and Hg–I distances are almost equal; thus the strong distortion in the tetrahedral environment of the four donor atoms is explained on the basis of strong stereo interactions between the two $\mathbf{L^1}$ ligands in each complex.

However, in crystal complex **2**, the ligand with two potential coordination nitrogen atoms, only one pyridine nitrogen atom of the ligand participates, coordinating to mercury(II). It does not present helices like the reported 2,2′- and 4,4′-bipyridyl-based "building block" compounds before. It is possible that the large volume of two iodine atoms repulses the ligands to form the very small angle of N–Hg–N [76.3(3)°], which produces strong stereo interactions when Hg^{II} ions bridge ligands to form the coordination polymer. The adjacent molecules are stacked to sheets through π–π interaction along the *b* axis with the short distance of 3.44 Å, and opposite sheets interact through pairwise C–H···I contacts [C–H···I = 3.92 Å, H···I = 3.16 Å][4] along the *c* axis, which have 2D sheets propagated as depicted in Figure 2 (b). Taking the van der Waals radii of H and I to be 1.20 and 2.15 Å, respectively, any H···I contact

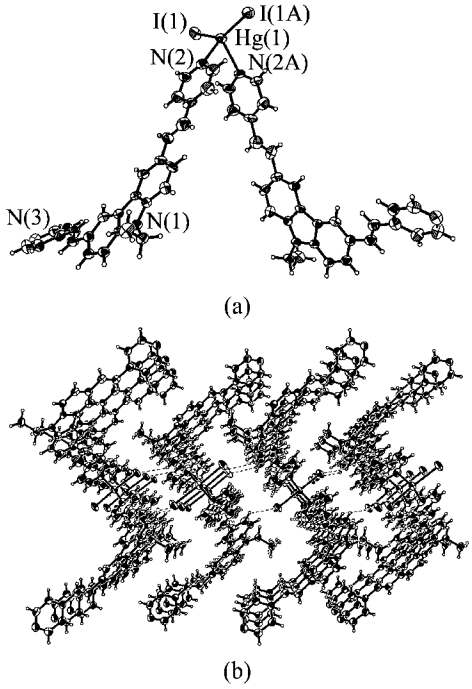

Figure 2. (a) Molecular structure and atom numbering of Hg-$(\mathbf{L^1})_2I_2$. The thermal ellipsoids are drawn at the 50% probability level. (b) Molecular packing of complex **2**.

Table 1. Selected intra- and intermolecular bond lengths [Å] and angles [°] for **1**–**4**.

1			
Hg(1)–N(2)	2.354(4)	N(3)–Hg(1)–N(2)	98.67(2)
Hg(1)–N(3)	2.299(4)	S(2)–Hg(1)–S(1)	127.06(6)
Hg(1)–S(2)	2.4371(2)	N(2)–Hg(1)–S(2)	101.00(1)
Hg(1)–S(1)	2.4493(2)	N(3)–Hg(1)–S(2)	107.89(1)
		N(3)–Hg(1)–S(1)	113.72(1)
		N(2)–Hg(1)–S(1)	103.49(1)
2			
Hg(1)–N(2)	2.425(6)	N(2)–Hg(1)–N(2A)	76.3(3)
		I(1)–Hg(1)–I(1A)	139.18(3)
Hg(1)–I(1)	2.6339(6)	N(2A)–Hg(1)–I(1A)	106.74(2)
		N(2)–Hg(1)–I(1A)	105.10(2)
3			
Hg(1)–N(2)	2.449(3)	N(3)–Hg(1)–N(2)	95.77(1)
Hg(1)–N(3)	2.336(4)	S(1)–Hg(1)–S(2)	126.19(5)
Hg(1)–S(1)	2.4510(2)	N(2)–Hg(1)–S(1)	101.63(1)
Hg(1)–S(2)	2.460(2)	N(3)–Hg(1)–S(1)	117.23(9)
		N(2)–Hg(1)–S(2)	103.30(9)
		N(3)–Hg(1)–S(2)	106.70(9)
4			
Hg(1)–N(2)	2.381(1)	N(3)–Hg(1)–N(2)	99.2(4)
Hg(1)–N(3)	2.447(1)	I(2)–Hg(1)–I(1)	128.51(6)
Hg(1)–I(2)	2.670(3)	N(2)–Hg(1)–I(1)	104.9(3)
Hg(1)–I(1)	2.674(2)	N(3)–Hg(1)–I(2)	103.5(3)
		N(3)–Hg(1)–I(1)	106.9(2)
		N(2)–Hg(1)–I(2)	110.1(2)

less than 3.35 Å and C–H···I angle >130° may therefore potentially be considered significant.[8] In complex **2**, the distance of H···I is 3.16 Å and the C–H···I angle is 152°, which indicate the formation of C–H···I hydrogen bonds. The importance of such C–H···I hydrogen bonds in supramolecular self-assembly has also been reported recently.[8] The overall structure is compact with small cavities.

Crystal Structure of $Hg_2(L^2)_2(SCN)_4$ (3)

The structure of complex **3** is shown in Figure 3 (a). The molecules of **3** exist as a centrosymmetric 30-membered macrometallacyclic ring formed by two $\mathbf{L^2}$ ligands bridging two Hg^{II} ions with pyridine nitrogen in *trans*-form. However, the macrocycle **3** is nonplanar and its cavity is large [N(2)–N(3A) = 12.713 Å, Hg(1)–Hg(1A) = 12.122 Å]; the dihedral angles between the pyridyl and carbazolyl rings, and the neighboring pyridyl ring are 31.6° and 20.2°, respectively. The opposite carbazolyl rings and pyridyl rings are parallel to each other.

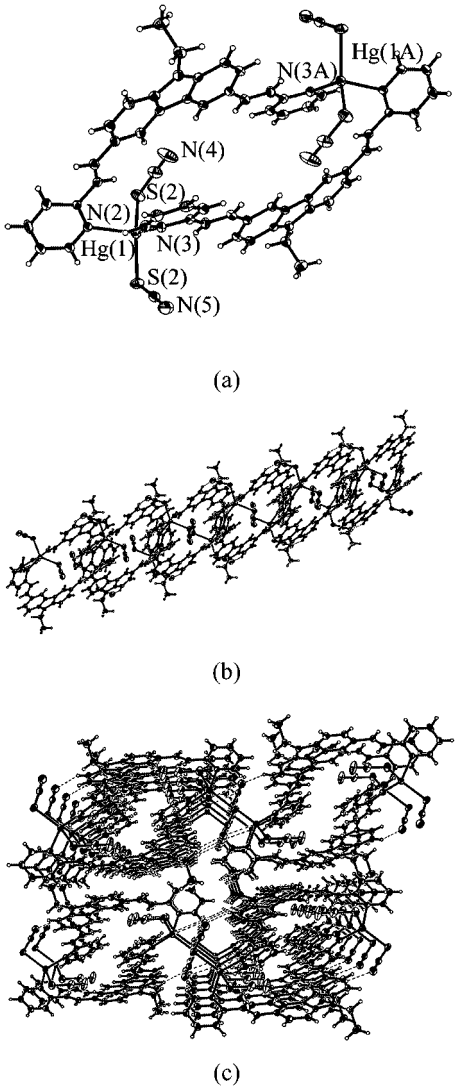

Figure 3. (a) Perspective view of the 30-membered macrometallacyclic ring of complex **3**. (b) The packing diagram of complex **3** showing π–π stacking interaction and the weak C–H···N interactions along the *b* axis. (c) The packing diagram of complex **3** between different chains showing the weak Hg···N interactions along the *c* axis.

In this complex, the $\mathbf{L^2}$ ligand has bidentate coordination, and each Hg^{II} center is coordinated by two pyridine nitrogen atoms from two different ligands and two sulfur atoms from two thiocyanate anions, showing a distorted tetrahedron geometry with a N–Hg–N bond angle of 95.77(1)°. The bond lengths of Hg–N_{av} of 2.39 Å and Hg–S_{av} of 2.455 Å fall within the expected values (Table 1). The dinuclear structures connect to each other through a π–π stacking interaction (the shortest distance of two macrocycles is 2.85 Å) and weak C–H···N interactions (C–H···N = 3.45 Å)[4] to form an infinite chain of macrocycles like a stair structure along the *b* axis (Figure 3, b). In particular, the difference chains (Figure 3, c) show some weak interaction through single, secondary Hg···N–C–S interactions (Hg···N = 3.59 Å) along the *a* axis. Together, the π–π stacking interaction and hydrogen bond form the overall two-dimensional network.

Crystal Structure of $[HgL^2I_2]_n$ (4)

Helical structures represent a longstanding synthetic target for the supramolecular chemist because of their intrinsic aesthetic appeal and potentially exploitable properties.[9] At this time, our attempts are directed toward the generation of a helical chain through the variation of the anion while maintaining the metal ion and ligand structure. The most striking feature of compound **4** is the interesting arrangement of $\mathbf{L^2}$ molecules and usual coordination of mercury atoms forming a unique helical structure. As described in Figure 4 (a), complex **4** also contains a pair of HgI_2 units and two $\mathbf{L^2}$ ligands in its asymmetric unit cell. However, these components do not connect to another to form a macrocyclic structure like complex **3**, but rather connect to form an infinite polymeric chain structure. A compact single-stranded helical chain is formed by self-assembly of $[HgL^2I_2]$ by coordination of *meta*-related peripheral pyridine-N of this unit to the neighboring Hg^{II} center running along a crystallographic 2_1 axis in the *a* direction with a long pitch of about 11.69 Å; at the widest point the diameter of the helix equals 6.13 Å.

In addition, like complex **1**,[7] the adjacent helical chains in compound **4**, one exhibiting left-handedness and the other right-handedness, are not entangled together but interact through π–π stacking interactions (the shortest distance of pyridyl and benzyl rings is 3.42 Å), which are alternatively offered by two helical chains to generate a compact double-stranded helical chain (Figure 4, b). To illustrate this clearly, the left- and right-handed helical chains are represented in Figure 4, b. Like complex **1**, these double-stranded helical chains are further extended into the two-dimensional architecture by C–H···I hydrogen bond interactions established between ligands and iodine anions of adjacent chains (C–H···I = 4.14 Å, H···I = 3.23 Å)[4] with interactions along the *b* axis in compound **4** (Figure 4, c). In complex **4**, the distance of H···I is 3.23 Å and the C–H···I angle is 142°, which indicate the formation of C–H···I hydrogen bonds. Because left-handed and right-handed helical chains coexist in the crystal structure, the whole crystal is mesomeric and does not exhibit chirality.

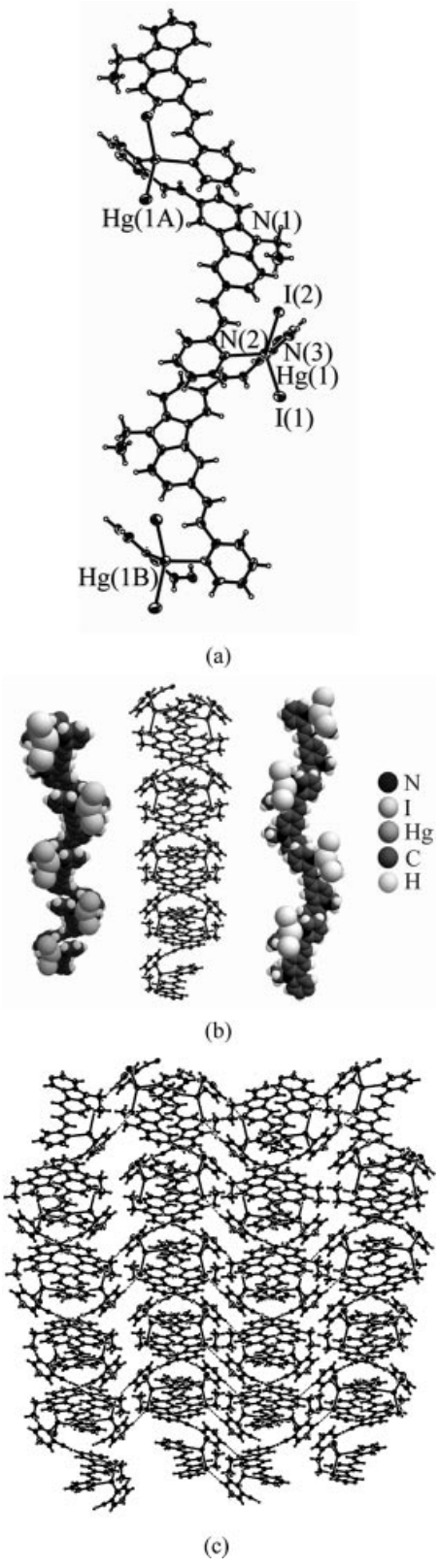

Figure 4. (a) Molecule structure of **4** showing different coordination environments of the two structurally independent Hg^{II} ions. (b) Space-filling plots of the right-handed chain (left), left-handed chain (right), and the ball-and-stick plot (middle) of the double helix bridged by a π–π stacking interaction in complex **4**. (c) Molecular packing of **4** viewed along the *b* axis by intermolecular hydrogen bond C–H···I.

In the present work, four different Hg^{II} coordination complexes **1**–**4** with bis(pyridyl) ligands (**L**^{1}, **L**^{2}) have been prepared and structurally characterized, giving metal–organic supramolecular architectures. Although compared with rigid bridging ligands, flexible bridging ligands are able to produce some unique frameworks with aesthetics and useful properties because of their flexibility and conformational freedom,[10] we designed and synthesized two novel functional rigid ligands with long conjugated chains that also present flexibility and conformational freedom to a certain extent. In complexes **1**–**4**, Hg^{II} centers all adopt four-coordination modes in different coordination environments. By comparing the structures of the four complexes, it is clear that the conformations of ligands in the complexes are related to the position of the nitrogen atom. Although complexes **1** and **3** have the same mercury(II) cation and thiocyanate counterion, ligand **L**^{1} of 4-N atoms in complex **1** takes on the *cis*-conformation to form helical chains and ligand **L**^{2} of 2-N atoms in complex **3** takes on the *trans*-conformation to form the macrometallacyclic ring; otherwise, ligand **L**^{1} of 4-N atoms in complex **1** and ligand **L**^{2} of 2-N atoms in complex **4** all take on the *cis*-conformation to form similar helical chains with nearly uniform bond lengths and angles (Table 1). Also, it should be noted that although **L**^{1}, with two potential coordination nitrogen atoms but only one pyridine nitrogen atom of the ligand, coordinates to mercury(II) in complex **2**, it is possible that the very small angle of N–Hg–N [76.3(3)°] produces strong stereo repulsion. This indicates that the conformations of ligands in the complexes may play an important role, indicating that the nature of the ligand is a determining factor in controlling the structural topology of these metal–organic supramolecular architectures, which offers the opportunity to control the coordination networks by ligand modifications.

Characterization

Thermogravimetric Analysis

The TG-DSC measurements of complexes **1**–**4** were determined in the range of 20–800 °C under nitrogen. To study the thermal stability of compounds **1**–**4**, thermal gravimetric analyses (TGA) were performed on the single crystal samples. TG data show that **1** is stable up to 235.2 °C, loses weight from 235.2 to 474 °C corresponding to decomposition of ligand **L**^{1}, and finally loses weight from 557 to 764 °C corresponding to the losses of $Hg(SCN)_2$. The TG data of **2** show that it is also stable up to 250 °C and then keeps losing weight from 250 °C to 768 °C, corresponding to decomposition of ligand **L**^{1} and HgI_2. The TG data for **3** show that it begins to decompose at 197 °C, then there are two weight-loss stages in the ranges 197–481 °C and 530–775 °C, corresponding to decomposition of ligand **L**^{2} and the losses of $Hg(SCN)_2$, respectively. The TG data of **4** show that the weight loss from 192 to 292 °C corresponds to the losses of ligand **L**^{2}, and the weight loss from 292 to 520 °C corresponds to decomposition of HgI_2.

Luminescent Properties

Luminescent transition-metal complexes containing multichromophoric ligands with extended conjugation have been extensively studied in recent years, partly because of their potential use as sensors, probes, and photonic devices.[11] Owing to the ability to affect the emission wavelength of organic materials, syntheses of inorganic–organic coordination complexes by the judicious choice of organic spacers and transition-metal centers can be an efficient method for obtaining new types of electroluminescent materials.[12] Free ligands **L**^{1} and **L**^{2}, and their metal complexes **1**–**4** show emission in solid state at room temperature (Figure 5). The nanosecond range of lifetime in the solid state at 298 K reveals that the emission is fluorescent in nature. The solid-state fluorescent analyses show that complexes exhibit different properties. As shown in Figure 5 (a), complex **1** exhibits an intense broad emission band centered at 608 nm, which is completely invariant to the excitation over the range of 300 to 534 nm and complex **2** always displays a weak broad emission band centered at 604 nm upon excitation over the range of 300 to 543 nm. These fluorescent emissions can be tentatively assigned to the ligand-to-metal charge transfer (LMCT), as two emissions at 452 and 522 nm upon excitation over the range of 300–428 nm can be observed for the free **L**^{1}. Complex **3** exhibits a broad

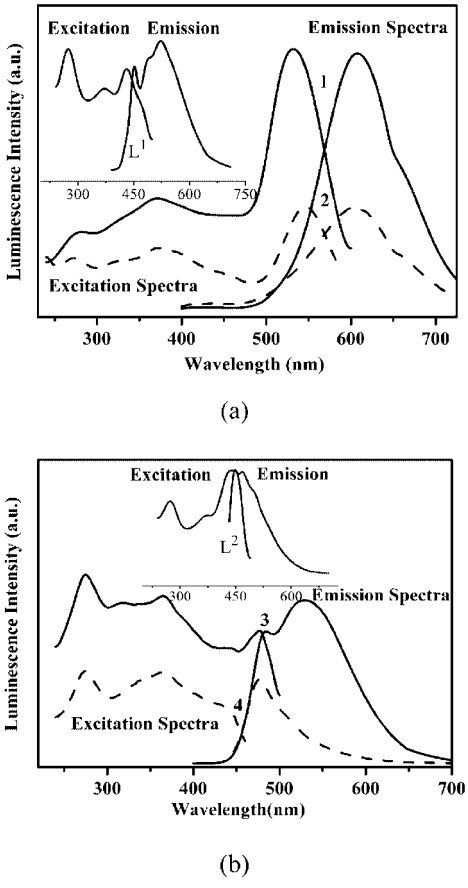

Figure 5. Solid-state emission spectra of complexes at room temperature: (a) **L**^{1}, **1**, and **2**; (b) **L**^{2}, **3** and **4**.

intense emission band at 528 nm with a shoulder at 484 nm upon excitation over the range of 365–477 nm, which can be tentatively assigned to LMCT and the intraligand fluorescent emission. However, complex **4** presents a sharp weak emission band with the maximum at 477 nm, which is completely invariant to the excitation over the range of 300–429 nm. The emission spectrum in complex **4** is largely characteristic of the intraligand fluorescent emission, as two emissions at 448 and 467 nm upon excitation over the range of 300 to 423 nm can be observed for the free $\mathbf{L^2}$. Thus the difference in the intense emission results from the different coordinated counteranions to Hg^{II} (I^- for **2**, **4** and SCN^- for **1**, **3**), which suggests that the change of counteranions has an important effect on their fluorescent property.[13]

Experimental Section

All chemicals and solvents were dried and purified by the usual methods. Elemental analyses were performed with a Perkin–Elmer 240C elemental analyzer. IR spectra were recorded with a Nicolet FTIR Nexus 870 instrument in the range 4000–400 cm^{-1} by using KBr pellets. The far-IR spectra (600–50 cm^{-1}) were recorded as Nujol mulls between polyethylene sheets. ^1H and ^{13}C NMR spectra were performed on a Bruker av600 MHz Ultrashield spectrometer and are reported as parts per million (ppm) from TMS (δ). The thermal behaviors were recorded with a Perkin–Elmer Pris-1 DMDA-V1 analyzer in N_2 at a heating rate of 5 °C min^{-1}. The luminescent spectra were measured on single crystals at room temperature using a Fluorolog-3-TAU steady-state/lifetime spectrofluorometer. The excitation slit was 2 nm, and the emission slit was 2 nm also.

X-ray Crystallography: Single-crystal X-ray diffraction measurements were carried out on a Bruker Smart 1000 CCD diffractometer equipped with a graphite crystal monochromator situated in the incident beam for data collection at room temperature. The determination of unit cell parameters and data collections were performed with Mo-K_α radiation (λ = 0.71073 Å). Unit cell dimensions were obtained with least-squares refinements, and all structures were solved by direct methods using SHELXL-97.[14] The other non-hydrogen atoms were located in successive difference Fourier syntheses. The final refinement was performed by full-matrix least-squares methods with anisotropic thermal parameters for non-hydrogen atoms on F^2. The hydrogen atoms were added theoretically and riding on the concerned atoms. Crystallographic crystal data and processing parameters for compounds **1**–**4** are shown in Table 2. Selected bond lengths and bond angles are listed in Table 1.

CCDC-245193 (for **1**), -245192 (for **2**), -241585 (for **3**), and -241588 (for **4**) contain the supplementary crystallographic data for this paper. These data can be obtained free of charge from The Cambridge Crystallographic Data Centre via www.ccdc.cam.ac.uk/data_request/cif.

Preparation of 9-Ethyl-3,6-diiodocarbazole: 9-Ethylcarbazole (10 g, 51 mmol) and anhydrous ethanol (150 mL) were added to a three-necked flask equipped with a magnetic stirrer, a reflux condenser, and an isobaric dropping funnel. ICl (20 g, 123 mmol)/ethanol (20 mL) was added to the mixture at 80 °C. The reaction mixture was refluxed for 2 h, cooled to room temperature and filtered. The grey needle crystals (20.52 g, 45.9 mmol) obtained (90%) were washed with ethanol. M.p. 154–155 °C. ^1H NMR (600 MHz, [D_6]-DMSO): δ = 1.27 (t, J = 6.6 Hz, 3 H), 4.41 (q, J = 6.6 Hz, 2 H), 7.50 (d, J = 8.4 Hz, 2 H), 7.74 (d, J = 8.4 Hz, 2 H), 8.61 (s, 2 H).

Preparation of 9-Ethyl-3,6-bis[2-(4-pyridyl)ethenyl]carbazole ($\mathbf{L^1}$): 9-Ethyl-3,6-diiodocarbazole (3.13 g, 7 mmol), potassium carbonate (2.42 g, 17.5 mmol), tetra-*n*-butylammonium bromide (2.26 g, 7 mmol), tri-*o*-tolylphosphane (0.21 g, 0.7 mmol), 4-vinylpyridine (4 mL, 30 mmol), palladium(II) acetate (0.047 g, 0.2 mmol) and redistilled *N*,*N*-dimethylformamide (7 mL) under nitrogen were added to a three-necked flask equipped with a magnetic stirrer, a reflux condenser and a nitrogen input tube. The reaction mixture was refluxed in an oil bath at 100 °C under nitrogen. The resulting solution was refluxed for 48 h and then cooled to room temperature. The residue was extracted with dichloromethane (600 mL), washed three times with distilled water, and dried with anhydrous magnesium sulfate. Then it was filtered and concentrated. The resulting solution was chromatographed over 200 g of silica gel. Elution with ethyl acetate and the recrystallization from ethanol produced light yellow crystals. Yield: 1.99 g (71%). M.p. 247.1–247.4 °C. ^1H NMR (600 MHz, [D_6]DMSO): δ = 1.35 (t, J = 6.9 Hz, 3 H), 4.49 (q, J = 6.9 Hz, 2 H), 7.29 (d, J = 16.3 Hz, 2 H), 7.59 (d, J = 4.8 Hz, 4 H), 7.69 (d, J = 8.4 Hz, 2 H), 7.74 (d, J = 16.3 Hz,

Table 2. Crystallographic data and structure refinement summary for complexes **1**–**4**.

Complex	**1**	**2**	**3**	**4**
Empirical formula	$C_{30}H_{23}HgN_5S_2$	$C_{56}H_{46}HgI_2N_6$	$C_{60}H_{46}Hg_2N_{10}S_4$	$C_{28}H_{23}HgI_2N_3$
Formula mass	718.24	1257.38	1436.49	855.88
Crystal system	monoclinic	monoclinic	monoclinic	monoclinic
Space group	$P2_1/c$	$C2/c$	$P2_1/n$	$P2_1/c$
a [Å]	8.2569(1)	34.732(7)	15.919(1)	8.468(9)
b [Å]	15.978(2)	8.4181(2)	8.119(6)	23.28(3)
c [Å]	21.205(3)	16.785(3)	21.663(2)	13.933(2)
β [°]	91.673(2)	98.698(3)	103.640(1)	98.012(2)
V [Å^3]	2796.4(7)	4851.0(17)	2721(3)	2719(5)
Z	4	4	2	4
D_{calcd} [g cm^{-3}]	1.706	1.996	1.753	2.091
θ range [°]	1.92–25.03	2.37–25.03	1.44–25.03	1.72–25.02
Total no. of data	14504	12284	13838	11579
No. of unique data	4940	4257	4811	4613
No. of parameters refined	343	295	343	307
R_1	0.0332	0.0407	0.0270	0.0574
wR_2	0.0686	0.0917	0.0630	0.1347
Gof	1.006	1.015	1.002	1.002

2 H), 7.83 (d, J = 8.4 Hz, 2 H), 8.52 (s, 2 H), 8.55 (d, J = 4.8 Hz, 4 H). ^{13}C NMR (600 MHz, [D$_6$]DMSO): δ = 150.43, 145.34, 140.83, 134.51, 128.16, 126.11, 123.63, 123.12, 121.06, 119.97, 110.32, 37.81, 14.31. IR (KBr): $\tilde{\nu}$ = 2927 (m), 2860 (w), 1729 (m), 1627 (m), 1600 (s), 1485 (m), 1413 (w), 1344 (m), 1233 (m), 1155 (w), 1126 (w), 1022 (w), 960 (m), 805 (m), 705 (m), 591 (w), 525 (w) cm^{-1}. $C_{28}H_{23}N_3$ (401.50): calcd. C 83.76, H 5.77, N 10. 47; found C 83.80, H 5.76, N 10.44.

Preparation of 9-Ethyl-3,6-bis[2-(2-pyridyl)ethenyl]carbazole (L^2): 9-Ethyl-3,6-diiodocarbazole (3.13 g, 7 mmol), potassium carbonate (2.42 g, 17.5 mmol), tetra-*n*-butylammonium bromide (2.26 g, 7 mmol), and 2-vinylpyridine (4 mL, 30 mmol) were dissolved in redistilled *N*,*N*-dimethylformamide (7 mL). Palladium(II) acetate (0.047 g, 0.2 mmol) and tri-*o*-tolylphosphane (0.21 g, 0.7 mmol) were added to it. The resulting solution was refluxed for 5 days and then cooled to room temperature. The residue was extracted with dichloromethane (600 mL), washed three times with distilled water, and dried with anhydrous magnesium sulfate. Then it was filtered and concentrated. The resulting solution was chromatographed over silica gel (200 g). Elution with ethyl acetate/petroleum ether (2:1) and the recrystallization from ethyl acetate produced light yellow crystals. Yield: 1.88 g (67%). M.p. 189.3–189.4 °C. ^{1}H NMR (600 MHz, [D$_6$]DMSO): δ = 1.35 (t, J = 7.2 Hz, 3 H), 4.48 (q, J = 7.2 Hz, 2 H), 7.24 (t, J = 6.0 Hz, 2 H), 7.36 (d, J = 16.2 Hz, 2 H), 7.57 (d, J = 7.2 Hz, 2 H), 7.66 (d, J = 7.2 Hz, 2 H), 7.80 (q, 4 H), 7.87 (d, J = 16.2 Hz, 2 H), 8.55 (s, 2 H), 8.59 (d, J = 4.2 Hz, 2 H). ^{13}C NMR (600 MHz, [D$_6$]DMSO): δ = 155.59, 149.50, 140.21, 136.81, 133.11, 127.87, 125.58, 125.44, 122.76, 121.91, 121.87, 119.53, 109.74, 37.31, 13.84. IR (KBr): $\tilde{\nu}$ = 2933 (m), 2866 (w), 1733 (m), 1626 (m), 1590 (s), 1488 (m), 1412 (w), 1385 (m), 1347 (w), 1236 (m), 1193 (w), 1160 (w), 1124 (w), 970 (m), 810 (m), 597 (w), 520 (w) cm^{-1}. $C_{28}H_{23}N_3$ (401.50): calcd. C 83.76, H 5.77, N 10.47; found C 83.72, H 5.78, N 10.50.[15]

Preparation of $[HgL^1(SCN)_2]_n$ (1): L^1 (40.01 mg, 0.1 mmol) in CH_2Cl_2 solution (5 mL) was layered onto a solution of $Hg(SCN)_2$ (31.6 mg, 0.1 mmol) in MeOH (5 mL) and stood for several days to give red single crystals of **1**. Yield 64.64 mg (90%). IR: $\tilde{\nu}$ = 2065 (vs), 419 (m), 327 (m). $C_{30}H_{23}HgN_5S_2$ (718.24): calcd. C 50.17, H 3.23, N 9.75; found C 50.14, H 3.24, N 9.77.

Preparation of $Hg(L^1)_2I_2$ (2): L^1 (40.01 mg, 0.1 mmol) in $CHCl_3$ solution (5 mL) was layered onto a solution of HgI_2 (45.4 mg, 0.1 mmol) in MeOH (10 mL) and stood for a week to give yellow single crystals of **2**. Yield 111.91 mg (89%). IR: $\tilde{\nu}$ = 420 (m), 151 (s). $C_{56}H_{46}HgI_2N_6$ (1257.38): calcd. C 53.49, H 3.69, N 6.68; found C 53.51, H 3.68, N 6.69.

Preparation of $Hg_2(L^2)_2(SCN)_4$ (3): L^2 (40.01 mg, 0.1 mmol) and $Hg(SCN)_2$ (31.6 mg, 0.1 mmol) were dissolved in MeOH (20 mL), refluxed for 2 h at 70 °C, and cooled to give a clear yellow solution. Yellow crystals suitable for X-ray diffraction were obtained after two weeks by slow evaporation of the methanol solution at room temperature. Yield 57.46 mg (80%). IR: $\tilde{\nu}$ = 2061 (vs), 420 (m), 328 (m). $C_{60}H_{46}Hg_2N_{10}S_4$ (1436.49): calcd. C 50.17, H 3.23, N 9.75; found C 50.14, H 3.24, N 9.77.

Preparation of $[HgL^2I_2]_n$ (4): L^2 (40.01 mg, 0.1 mmol) and HgI_2 (31.6 mg, 0.1 mmol) were dissolved in MeOH (20 mL), refluxed for 2 h at 70 °C, and cooled to room temperature giving a clear yellow solution. Pale yellow crystals suitable for X-ray diffraction were obtained after several days by slow evaporation of the methanol solution at room temperature. Yield 77.89 mg (91%). IR: $\tilde{\nu}$ = 419 (m), 151 (s). $C_{28}H_{23}HgI_2N_3$ (855.88): calcd. C 39.29, H 2.71, N 4.91; found C 39.28, H 2.72, N 4.92.

Acknowledgments

We thank the National Natural Science Foundation of China (50272001, 50335050, 50532030), and Person with Ability Foundation of Anhui Province 2002Z021. We also wish to thank Prof. D. Q. Wang of University of Liao Cheng for his assistance with the X-ray structure determinations.

[1] a) J. S. Evans, R. L. Musselman, *Inorg. Chem.* **2004**, *43*, 5613–5629; b) Z. Q. Qin, M. C. Jennings, R. J. Puddephatt, *Inorg. Chem.* **2001**, *40*, 6220–6228; c) B. Moulton, M. J. Zaworotko, *Chem. Rev.* **2001**, *101*, 1629–1658; d) K. Kim, *Chem. Soc. Rev.* **2002**, *31*, 96–107; e) S. Sailaja, M. Rajasekharan, *Inorg. Chem.* **2003**, *42*, 5675–5684.

[2] a) M. L. Tong, X. M. Chen, B. H. Ye, L. N. Ji, *Angew. Chem. Int. Ed.* **1999**, *38*, 2237–2240; b) M. Eddaoudi, H. Li, O. M. Yaghi, *J. Am. Chem. Soc.* **2000**, *122*, 1391–1397; c) K. S. Min, M. P. Suh, *J. Am. Chem. Soc.* **2000**, *122*, 6834–6840; d) J. Y. Lu, A. M. Babb, *Inorg. Chem.* **2001**, *40*, 3261–3262; e) A. Fu, X. Huang, J. Li, T. Yuen, C. L. Lin, *Chem. Eur. J.* **2002**, *8*, 2239–2247; f) M. L. Tong, Y. M. Wu, J. Ru, X. M. Chen, S. Kitagawa, *Inorg. Chem.* **2002**, *41*, 4846–4848; g) D. M. Shin, I. S. Lee, Y. K. Chung, *Inorg. Chem.* **2003**, *42*, 8838–8848; h) X. H. Bu, Y. B. Xie, J. R. Li, R. H. Zhang, *Inorg. Chem.* **2003**, *42*, 7422–7430; i) T. J. Burchell, D. J. Eisler, R. J. Puddephatt, *Inorg. Chem.* **2004**, *43*, 5550–5557; j) S. Mukhopadhyay, P. B. Chatterjee, D. Mandal, G. Mostafa, A. Caneschi, J. V. Slageren, T. J. R. Weakley, M. Chaudhury, *Inorg. Chem.* **2004**, *43*, 3413–3420; k) H. Zheng, H. B. Song, M. Du, Sh. T. Chen, X. H. Bu, *Inorg. Chem.* **2004**, *43*, 931–944.

[3] a) S. K. Ghosh, P. K. Bharadwaj, *Inorg. Chem.* **2004**, *43*, 2293–2298; b) T. P. Losier, M. J. Zaworotko, *Angew. Chem. Int. Ed. Engl.* **1996**, *35*, 2779–2782; c) K. N. Power, L. Hennigar, M. J. Zaworotko, *Chem. Commun.* **1998**, 595–596; d) P. J. Hagrman, D. Hagrman, J. Zubieta, *Angew. Chem. Int. Ed.* **1999**, *38*, 2638–2684; e) Z. Q. Qin, M. C. Jennings, R. J. Puddephatt, *Inorg. Chem.* **2002**, *41*, 5174–5186; f) T. Akutagawa, T. Nakamura, *Coord. Chem. Rev.* **2003**, *226*, 3–81; g) Y. B. Dong, P. Wang, R. Q. Huang, *Inorg. Chem.* **2004**, *43*, 4727–4739.

[4] a) A. M. Beatty, *Coord. Chem. Rev.* **2003**, *246*, 131–143; b) H. W. Roesky, M. Andruh, *Coord. Chem. Rev.* **2003**, *236*, 91–119.

[5] H. J. Hoegl, *Phys. Chem.* **1965**, *69*, 755–759.

[6] a) M. He, R. J. Twieg, U. Gubler, D. Wright, W. E. Moerner, *Chem. Mater.* **2003**, *15*, 1156–1164; b) K. R. Justin Thomas, J. T. Lin, Y. T. Tao, Ch. H. Chuen, *Chem. Mater.* **2002**, *14*, 3852–3859; c) B. Liu, L. W. Yu, Y. H. Lai, W. Huang, *Chem. Mater.* **2001**, *13*, 1984–1991; d) Ch. W. Ko, Y. T. Tao, J. T. Lin, K. R. Justin Thomas, *Chem. Mater.* **2002**, *14*, 357–361; e) H. Chun, I. K. Moon, D. H. Shin, N. Kim, *Chem. Mater.* **2001**, *13*, 2818–2823.

[7] a) Ch. Y. Su, A. M. Goforth, M. D. Smith, H. C. Z. Loye, *Inorg. Chem.* **2003**, *42*, 5685–5692; b) T. J. Burchell, D. J. Eisler, R. J. Puddephatt, *Inorg. Chem.* **2004**, *43*, 5550–5557.

[8] a) C. J. Horn, A. J. Blake, N. R. Champness, A. Garau, V. Lippolis, C. Wilson, M. Schröder, *Chem. Commun.* **2003**, 312–313; b) L. Y. Kong, Zh. H. Zhang, T. A. Okamura, M. J. Fei, W. Y. Sun, N. Ueyama, *Chem. Lett.* **2004**, *12*, 1572–1573.

[9] a) P. A. Maggard, C. L. Stern, K. R. Poeppelmeier, *J. Am. Chem. Soc.* **2001**, *123*, 7742–7743; b) Z. Shi, S. H. Feng, S. Gao, L. R. Zhang, G. Y. Yang, J. Hua, *Angew. Chem. Int. Ed.* **2000**, *39*, 2325–2326; c) C. Z. Lu, C. D. Wu, S. F. Lu, J. C. Liu, Q. J. Wu, Q. J. Hui, H. H. Zhuang, J. S. Huang, *Chem. Commun.* **2002**, 152–153; d) Y. Wang, J. H. Yu, M. Guo, R. R. Xu, *Angew. Chem. Int. Ed.* **2003**, *42*, 4089–4092; e) M. C. Hong, W. P. Su, R. Cao, M. Fujita, J. X. Lu, *Chem. Eur. J.* **2000**, *6*, 427–431; f) X. H. Bu, H. Liu, M. Du, L. Zhang, Y. M. Guo, M. Shionoya, J. Ribas, *Inorg. Chem.* **2002**, *41*, 5634–5634; g) J. Vinje, J. A. Parkinson, P. J. Sadler, T. Brown, E. Sletten, *Chem.*

Eur. J. **2003**, *9*, 1620–1630; h) Z. Wu, Q. Chen, S. Xiong, B. Xin, Z. Zhao, L. Jiang, J. S. Ma, *Angew. Chem. Int. Ed.* **2003**, *42*, 3271–3274; i) M. Barboiu, G. Vaughan, R. Graff, J. M. Lehn, *J. Am. Chem. Soc.* **2003**, *125*, 10256–10265.

[10] a) M. Du, X. H. Bu, Z. Huang, S. T. Chen, Y. M. Gao, *Inorg. Chem.* **2003**, *42*, 552–559; b) X. H. Bu, W. Chen, S. T. Lu, R. H. Zhamg, D. Z. Liao, W. M. Bu, M. Shionoya, F. Brisse, J. Ribas, *Angew. Chem. Int. Ed.* **2001**, *40*, 3201–3203; c) F. A. Paz, Y. Z. Khimyak, A. D. Bond, J. Rocha, J. Klinowski, *Eur. J. Inorg. Chem.* **2002**, 2823–2828; d) Y. B. Dong, M. D. Smith, R. C. Layland, H. C. zur Loye, *Inorg. Chem.* **1999**, *38*, 5027–5033.

[11] a) Sh.-Sh. Sun, A. J. Lees, *Coord. Chem. Rev.* **2002**, *230*, 170–191; b) V. Balzani, A. Juris, M. Venturi, S. Campagna, S. Serroni, *Chem. Rev.* **1996**, *96*, 759–834.

[12] a) D. M. Ciurtin, N. G. Pschirer, M. D. Smith, U. H. F. Bunz, H. C. zur Loye, *Chem. Mater.* **2001**, *13*, 2743–2745; b) E. Cariati, X. Bu, P. C. Ford, *Chem. Mater.* **2000**, *12*, 3385–3391; c) F. Würthner, A. Sautter, *Chem. Commun.* **2000**, 445–446.

[13] Y. Q. Gong, R. H. Wang, Y. F. Zhou, D. Q. Yuan, M. Ch. Hong, *J. Mol. Struct.* **2005**, *705*, 29–33.

[14] G. M. Sheldrick, *SHELXL-97, Program for Crystal Structures Refinement*, University of Göttingen, Göttingen, Germany, **1997**.

[15] H. P. Zhou, J. Zh. Zhang, D. M. Li, Y. M. Zhu, Zh. J. Hu, J. Y. Wu, Y. Xie, M. H. Jiang, X. T. Tao, Y. P. Tian, *J. Mol. Struct.* **2005**, *743*, 93–97.

Received: May 16, 2005
Published Online: October 27, 2005

